

PAPER • OPEN ACCESS

Dynamic measurements on a Kaplan turbine: model – prototype comparison

To cite this article: M Angulo *et al* 2019 *IOP Conf. Ser.: Earth Environ. Sci.* **240** 022006

View the [article online](#) for updates and enhancements.

Dynamic measurements on a Kaplan turbine: model – prototype comparison

M Angulo¹, C Lucino¹, F Botero², A Rivetti¹, S Liscia¹

¹Laboratorio de Hidromecánica, Facultad de Ingeniería, Universidad Nacional de La Plata, 47 N° 200, La Plata, Argentina.

²Mecánica Aplicada, Escuela de Ingeniería, Universidad EAFIT, Carrera 49 N° 7 Sur - 50, Medellín, Colombia

e-mail: cecilia.lucino@gmail.com

Abstract. The purpose of this paper is to validate in prototype, the results related to the description of dynamic behaviour obtained in a Kaplan turbine model. A comparative analysis between model and prototype measurement at homologous operation conditions is presented. The phenomena of interest are tip vortex cavitation development and rotor stator interaction (rsi), associated to operation at high power outputs. The selection of suitable signal processing tools allows a clear identification of the role played by the modulation of the main rsi frequencies on cavitation phenomena. The comparison between pressure acceleration measurements on model and prototype at draft tube wall are consistent, both in time and frequency domain analysis. The acceleration measurement at the draft tube wall (manhole) is suggested as a trustworthy dynamic indicator for prediction (model) and monitoring (prototype) purposes.

1. Introduction

In a previous paper [1] a methodology for the evaluation of hydrodynamic behavior of Kaplan turbines was introduced. An experimental layout (including the instrumental consisting of accelerometers and a hydrophone) for physical models was proposed and tested. The location of the sensors, sampling characteristics and signal processing before mentioned are capable of describing the dynamic response of the turbine.

Tip blade cavitation plays an important role in the dynamic response of the machine, especially at high loads. The most harmful effects that can occur are excessive vibration level, cavitation erosion on the blades and, in some cases, the structural integrity of the discharge ring can also be compromised. These damages impact on maintenance costs and eventually also on the productivity of the plant because of power output limitations to preserve the units. In this paper, measurements on a prototype of a large Kaplan turbine are compared to the corresponding model operation points in order to explore the representability of the methodology proposed.

Pressure pulsations, vibration and acoustic emission can account for the nature and degree of aggressiveness of the cavitation and its incipient Sigma condition with particular sensitivity in model tests, provided that the sampling frequency and signal processing techniques are appropriately chosen. An adequate processing of dynamic signals allows detection of other phenomena of interest as well, like the modulation by typical frequencies, i.e. the passage of the blades and the corresponding rotor – stator interaction phenomena.

Although the question of scalability of dynamic behavior from model to prototype needs to be carefully studied, it is possible to get a good diagnosis of hydrodynamic phenomena in model for predictive purposes, since it has been proved its validity by means of measurements on prototype turbines of high output, homologous to the models tested, as it is described in this article. The study was carried out under the framework of a project focused on the dynamic behavior of Kaplan turbines that combines prototype measurements, model tests and CFD simulations,



and is supported by the Yacyretá Binational Entity (EBY) and the National University of La Plata, Argentina (UNLP). The motivation for the study is the presence of severe cavitation erosion at the discharge ring of the 20 units, in which 24 erosion patches were clearly distinguished, in coincidence with the number of wicket gate vanes. As previously shown [1] blade passage and rsi phenomena both modulate acceleration signal of transducers located at model draft tube wall and a hydrophone as well. It was proved that the arising of rsi manifestation in the model is associated to tip vortex cavitation development for high load operation conditions. Since the range of hydraulic frequencies that drive this phenomena are adequately represented by similarity laws in reduced scale model tests, the comparisons between model and prototype dynamic behavior is done in frequency domain. Dominance of this frequencies in spectral analysis reveals whether the phenomena arises in model and prototype, even when amplitude values cannot be scaled up because of the lack of similitude of masses.

2. Methods and materials

2.1. Measurements on the physical model

Experiments were performed at the Laboratory of Hydromechanics of the National University of La Plata, Argentina. The test rig is a closed circuit that allows for the testing of Kaplan and Francis turbines (figure 2). The model test was carried out in compliance with the IEC 60193 standard [2]. The error estimated for the hydraulic efficiency is less than 0.24 %.

The scale model is a five-blade Kaplan turbine with twenty-four stay and guide vanes. Its diameter is $D = 340$ mm and its specific speed $n_s = 614$. The rotational speed during the test is $n = 1000$ rpm, which yields a Reynolds number $Re = 6.05 \times 10^6$, based on the blade tip velocity. The model is placed in the test rig between the high- and low-pressure tanks. The head is adjusted by varying the rotational speed of the recirculation pump. The low-pressure tank is equipped with a vacuum pump and a pneumatic controlled valve allowing for the variation of the absolute pressure of the system, in order to set the desired Sigma cavitation number σ , given by equation (1).

$$\sigma = \frac{\left(\frac{p_b - p_v}{\gamma}\right) + h_s + Ec_2}{H} \quad (1)$$

where p_b = pressure at low-pressure tank, p_v = vapor pressure, γ = water specific weight, h_s = suction head, H = net head, Ec_2 = kinetic energy at the draft tube outlet. Given that the test was carried out at constant head, flow rate and rotational speed, it becomes apparent from equation 1 that can be modified only by varying the pressure at the low pressure tank.

2.1.1. Monitoring system. The accelerometer AC1 is located above the centerline of the runner; the AC2, $0.19 D_p$ below the blade passage plane and AC3, at the draft tube inlet. The hydrophone was located downstream the center-line at a distance of $1.0 D$ immersed in water. An inductive key phasor together with a cog was installed in the shaft to obtain the runner passage key (figure 2). Technical specifications of all the instruments are presented in table I, even though only AC2 registers are considered in this paper.

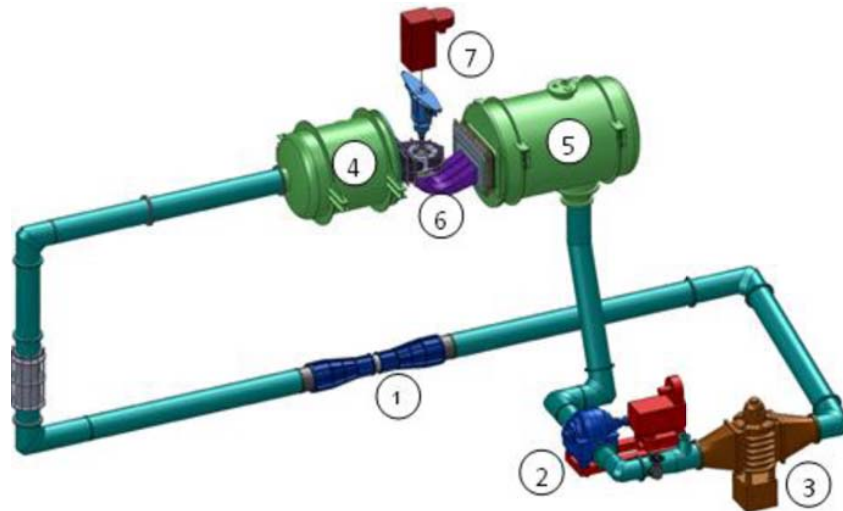


Figure 1. Test rig facility at the Laboratory of Hydromechanics of La Plata, Argentina. (1) Venturi flow-meter; (2) Recirculation pump; (3) Dissipation valve; (4) High-pressure tank; (5) Low-pressure tank; (6) Model scale; (7) Motor-generator.

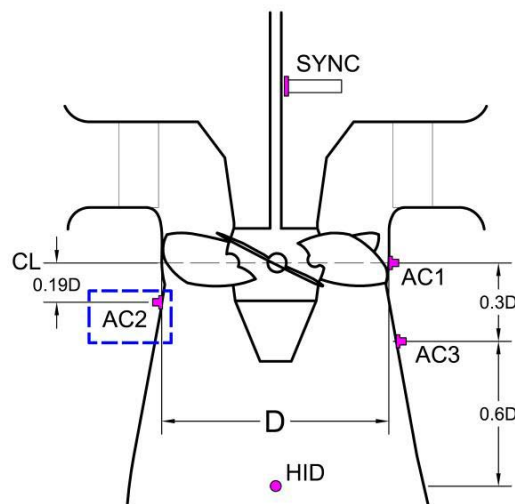


Figure 2. Instrumentation location on the Kaplan model scale. Accelerometer AC2 signal is analyzed in this paper.

2.2. Measurements on the prototype

Measurements have been done on a five-blade, 9.5-meter-diameter Kaplan turbine of the Yacyretá power station located on the Paraná river, at the border between Argentina and Paraguay. The power plant has an installed capacity of 3100 MW ($P_i = 155$ MW per unit) and operates on a range of heads between 19.5 m and 24.1 m. The rotational velocity of the turbine is 71.42 rpm and its head at the best efficiency point (BEP) is 28 m. The stator has 24 guide and stay vanes. The runner blades have an anti-cavitation lip and the stainless-steel discharge ring extends $0.153 D_p$ downstream from the runner centerline, D_p being the diameter of the runner.

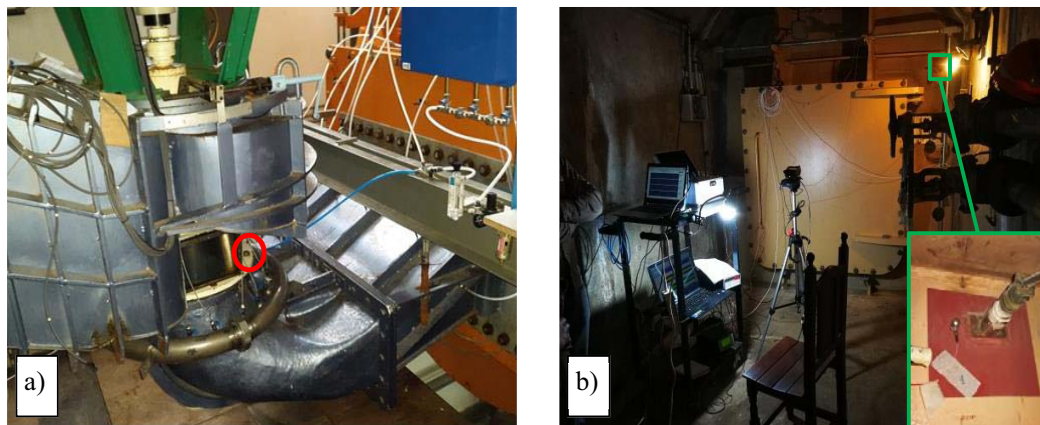


Figure 3: Instrumentation location of the accelerometer on model scale (a) and prototype scale (b). Location of accelerometer at the prototype corresponds to location of “AC3” in the model.

Table 1. Instruments technical specifications

Instrument	Nomenclature	Characteristics	Prototype	Model
Accelerometer #2	AC2	Brand	Wilcoxon Research	Endevco
		Model	793L	7259B-100
		Position	Discharge ring ¹	Discharge ring ²
		Range	+/- 10 g	+/- 50 g
		DA frequency	4,200 Hz	35,000 Hz
		Res. freq.	15 kHz	90 kHz
Data Acquisition system	DAS	Brand	NI	NI
		Model	SCXI-1600 USB	USB-6210
		Inputs	352 analog	16 analog
		Resolution	16 bits	16 bits
		DA frequency	200 kS/s	250 kS/s

¹ 0.30 D_p downstream the runner centerline

² 0.19 D_p downstream the runner centerline

2.3 Operation conditions tested at model and prototype

Four plant operation points were selected at $H/H_{nom}=0.97$, which can be seen on the hill diagram in figure 4. For the model tests, cavitation development corresponds to Sigma Plant value at each operation point.

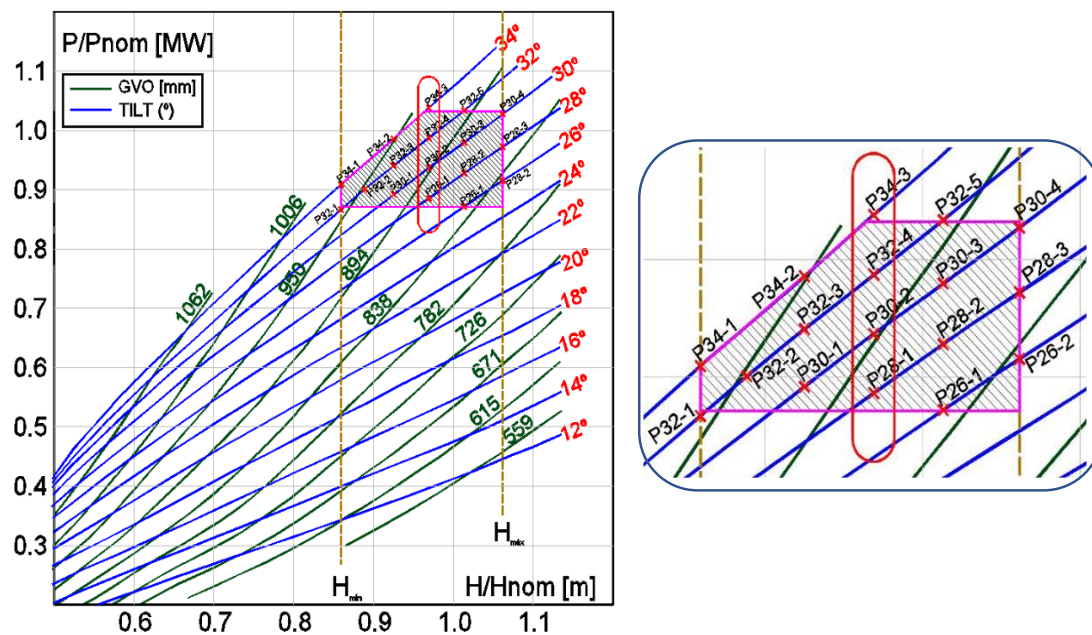


Figure 4. Operation points tested on dimensionless hill diagram.

2.4 Data processing

2.4.1 Time domain. The suitable selection of sensors and their location play a major role in the diagnostic assessment of tip vortex cavitation. Said phenomenon leaves a trace that can be unveiled both in time and frequency domains. On the one hand, the proper parameters of the turbine design influencing the formation of vortices, such as number of blades, blade clearance and discharge ring, and permissible tolerances for manufacture, are responsible for the behavior of the spectral components associated with rotor stator frequencies. The formation and subsequent implosion of clouds of vapor cavities become a source of wide-band noise. In addition, interactions among them and the between fluid and structure (FSI) provide a plentiful mine to be exploited [3].

The time-domain analysis for rotating turbomachinery can provide meaningful geometric and synchronous information if it is assumed that samples came from normal distributions; i.e., normal variables. In that sense, two types of strategies are proposed: inter-condition and condition-dependent analysis.

Traditional estimators such as the variance (equation (2)) and the root mean square value (rms, equation (3)), provide an overall measure of the variable x that can serve as an indicator for comparing different operating conditions. In fact, they indicate if the variable increases or decreases, globally, when the machine goes from one condition to the next (inter-condition). Here, x is understood as a series of N samples, successive, equally spaced and indexed in time order; each sample denoted by x_i . In the particular case of time series of zero mean ($\bar{x} = 0$), the rms value is equivalent to the standard deviation, which in turn is the square root of the variance.

$$var = \frac{1}{N-1} \sum_{i=1}^N (x_i - \bar{x})^2 \quad (2)$$

$$rms = \sqrt{\frac{1}{N} \sum_{i=1}^N x_i^2} \quad (3)$$

An estimation of the mean behavior of a random variable, during one shaft's revolution, can be obtained

averaging several (more than thirty) phased time-series samples of one revolution [4]. A review of Time Synchronous Average (TSA) algorithms was published by Bechhoefer and Kingsley [5]. Concisely, in our work it consists of: key phasor marks are used to index the time-ordered samples corresponding to one revolution length. An estimation of the variance is recovered by calculating the sample variance of the same set of time series (several revolutions of the rotor). Then a representation of the average revolution bounded by its confidence intervals can be plotted as a function of time, angular position or any other scale.

Balanced fluctuations with constant variance are expected from a machine in good condition; if strong bumps or fluctuations in variance are observed, it is a sign of defects located on the rotor oriented according to the horizontal scale used for the plot and the key phasor mark (condition-dependent analyses). Protuberances with low or constant variances can be explained by hydraulic, mechanical or electrical synchronized imbalances. High variance can be associated to stochastic phenomena like cavitation formation and implosion.

2.4.2. Frequency domain. Once cavitation incepts, the generated wide-band noise propagates from the collapsing bubbles, through the fluid, to the structure. This noise can be perceived as a global increase of the rms value of the collected signal, as stated above, but also as an energy pattern that emerges over several thousand Hertz; i.e. wide-banded. For this reason, conventional representations in the frequency domain as the amplitude spectrum or the power spectrum are not the best tools for the detection of cavitation. In general, such analyzes are not suitable for the technical diagnosis of stochastic phenomena.

Therefore, assuming that the dynamic transducer is installed in the stationary frame of a Kaplan turbine, then the recorded noise intensity coming from a cavitating vortex attached to the tip of the rotating runner blades varies periodically depending on the distance measured from the tip of the blade to the monitoring point. That is to say, the noise emitted by the implosion of the bubbles becomes more and less intense in a harmonic way, as the rotating blade with the anomaly approaches or moves away from the sensor.

This sort of modulation has two desirable characteristics that can be profit from the technical point of view: the first one is that instead of only one carrier frequency, there is a wide band of carrier frequencies; the second is that carrier frequencies may extend up to the highest sampled frequency. In other words, the information is carried by several frequency channels, and many of these channels are free of interference produced by other sources since their frequencies are high enough (several thousand hertz). Consequently, there are bands in the frequency domain where symptoms of tip vortex cavitation are preserved.

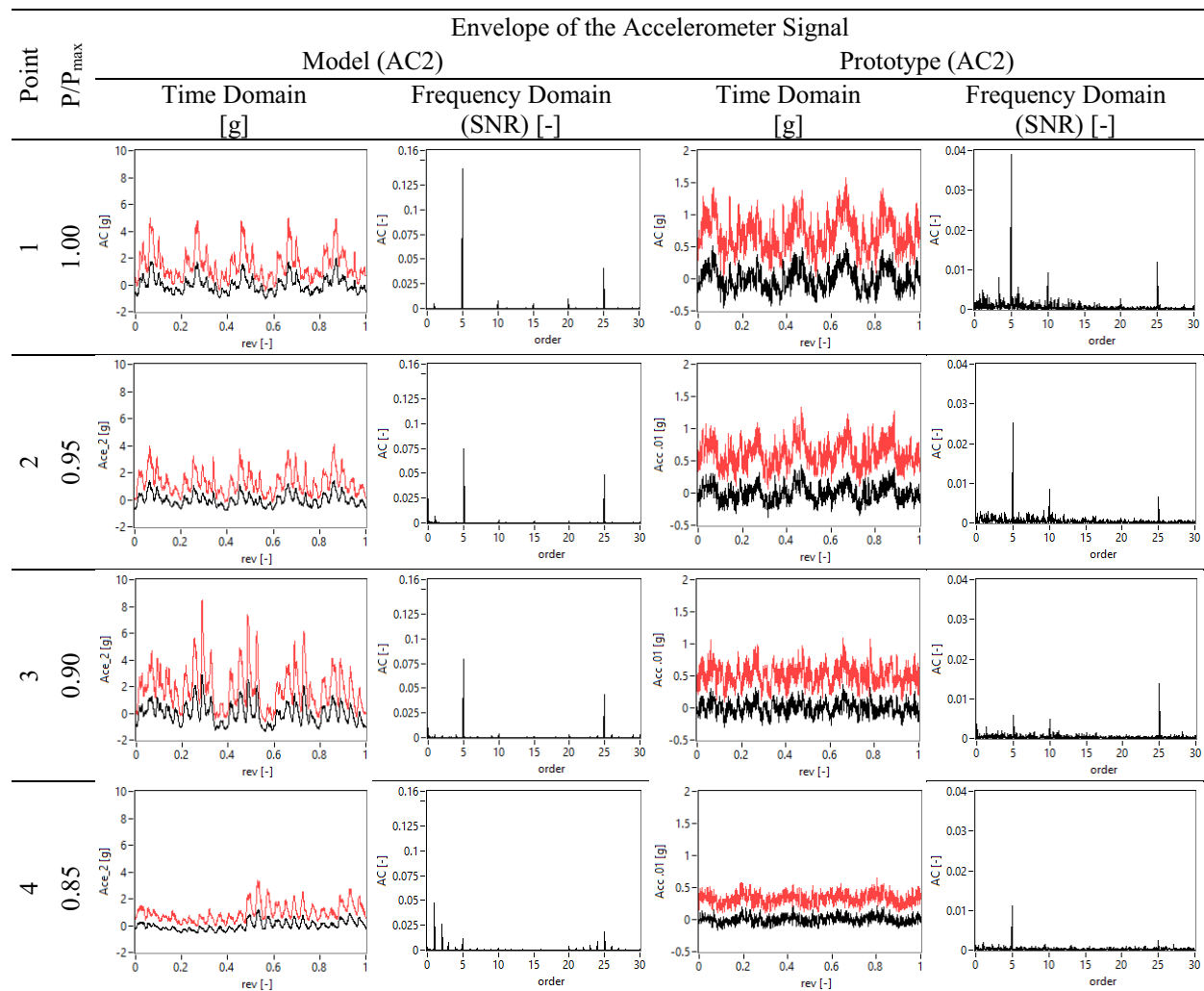
The demodulation technique described by Escaler et al. [6] is adopted to process the fluid and structure-borne. This technique has proven to be successful in diagnosing other manifestations of cavitation [7]. A more detailed description has been provided in the previous paper [1]. Spectral amplitudes are presented as the sound-to-noise ratio (SNR, equation 4) for comparative purposes; P_i and rms_i stand for the power and rms value of the i th spectral component while P_{noise} and rms_{noise} are the global power and rms value of the signal.

$$SNR_i = \frac{P_i}{P_{noise}} = \left(\frac{rms_i}{rms_{noise}} \right)^2 \quad (4)$$

It is expected that in the presence of tip vortex cavitation the most prominent frequency component corresponds to the passage of blades or one of its harmonics. On the contrary, a flat or decadent spectrum is anticipated.

3. Results

From the several variables registered, accelerometer signal located on draft tube wall, indicated in figure 2 as AC2, is analyzed in this paper (see details in table 1). The data collected with the accelerometer were demodulated following the procedure previously described and presented in a specific way. Each envelope was spectrally decomposed and the domain normalized with the frequency of shaft of the machine to be presented as orders of that frequency. The results of applying the introduced TSA procedure to the envelope of acceleration signal (draft tube wall) are presented in table 2 for both the model and the prototype. Black lines represent TSA values and red lines the added variance; here, the horizontal axis represents one revolution of the runner (normalized), while the vertical axis is expressed in gravities. Together with each time series graph, FFT of the envelope are also presented in table 2; both axes represent dimensionless quantities: the vertical axis corresponds to the signal-to-noise ratio (SNR) and the values on the horizontal axis are multiples of the rotation speed of the runner.

Table 2. Model and prototype results

For the model, from the lowest power output up to the highest one (0,85 up to 1,0), TSA values evolve towards a better definition of blade passage frequency (five peaks corresponding to 5 blades), value which is better appreciated in the FFT graphs, where the order 5 consistently grows. This means that high frequencies (identified with cavitation) are modulated by blade passage frequency. The rsi frequency $25f_n$ appears on the TSA curves along the range of outputs, but it is greater at $P/P_{\max}=0,80$ and higher outputs. Besides, the variance associated to each angular position (order of time in the horizontal axis) expresses the degree of dispersion of the envelope of the acceleration at that particular angular position. The contribution that is made by superimposing the variance is evident; for each blade passage at least the twenty-fifth synchronous component is identified. It is worth mentioning the fluctuation of the variance amplitude and its large magnitude compared to the average value of the acceleration.

For the prototype, TSA values (table 2) show the presence of blade passage frequency as the main modulating frequency along the whole range of outputs. Modulation from interaction frequency is more evident at higher outputs ($25f_n$). In this case, the variance shows more uniformity in time domain for all the points tested. Dispersion

above the envelope average value of the acceleration is more uniform in time domain compared to the model response.

4. Discussion

The dimensionless estimator used to represent the spectral amplitudes (SNR) is proposed as a very convenient alternative for the comparison of oscillating quantities from model to prototype. The amplitude of each component represents the contribution that it makes to the totality of the recovered information. In fact, taken into account that model masses do not fulfill dynamic similarity requirements, the presence of characteristic hydraulic frequencies, and their relative importance in the spectral diagram, are the variables of interest to explore through the processing of the instantaneous acceleration. Although relatively low values are always expected ($\ll 1$), we consider that SNR values above 0.01 should be carefully examined. Interestingly, in the results presented for the accelerometer, the envelope of the acceleration, for an equivalent monitoring point on the model and prototype, there is a four times higher contribution of the rsi frequencies in model tests, which is very encouraging for its use as a predictor. More research must be carried out to evaluate the performance of other dynamic quantities such as fluctuations in pressure, sound, etc.

The vibration modulation is present both in the model and in the prototype, every time a stochastic phenomenon, as the collapse of vapor cavities, overcomes a periodic phenomenon, such as a cavitating tip blade that approaches and moves away to the installation point of the accelerometer. The same happens with rsi phenomena, as previously described [1]. However, size dependent quantities such as the diameter of the impeller and the gap of the blade tip can affect the attenuation of the signal (which depends mainly on the distance, the frequency and the medium). It is for this reason that a better noise-to-signal ratio was measured for the scale model; i.e. lower distances and therefore acoustic energy losses. It is also important to clarify that the methodology as presented in this work allows the detection of tip vortex cavitation without addressing its effectiveness in predicting the dynamic forces that govern it.

On the other hand, the average representation of the envelopes in time domain do not suggest such an obvious comparison. Plots for model tests are much clearer than those for prototype measurements. An explanation for this effect is attributed to the tuning of the filtering required by the methodology. For the current results, cutting frequencies were established as orders of the rotation speed of the respective impeller. This can have a significant impact because when the rotational speeds of the model and prototype are very different, the wide bands of carrier frequencies for demodulation purposes are as well. The suggested alternative for future research is to set a sufficiently high sampling frequency, and from this, to define the filtering frequencies, which in this case will be the same for the model and the prototype.

Model and prototype both show a similar response in terms of modulation frequencies of the acceleration, corresponding to blade passage and rotor stator interaction. The origin of rsi modulating phenomena [1] is the interaction of tip cavitation volume with guide vanes wakes. One important impact of this phenomena is the erosion due to cavitation collapse at fixed spots over the discharge ring [7]. The location of these spots and the dynamics of each cavity depend of the rotational speed ω , and the number of guide vanes (Z_0) and runner blades (Z_b). The influence of the non-uniform flow leaving the guide vanes can be identified by the analysis of the modulation process generated by the stationary flow field of the 24 guide vanes, and the rotating flow field due to the 5 runner blades. The characteristic frequency of $25 f_n$, given by the expression $f/f_n = mZ_b$, has to be present if the interaction exists [1].

For the prototype, there are also more other low frequencies modulating the acceleration. This makes the TSA to look “noisy” than its homologous point at the model. The lower and less variable variance at the prototype seems to be related to the scale. In other words, in the model, dispersion is expected to be amplified compared to the prototype.

5. Conclusions

It has been demonstrated with prototype measurements the reliability of the methodology previously presented to describe dynamic response in the model of a Kaplan turbine. Demodulation analysis looks for the hydraulic driven forces that govern tip vortex cavitation evolution, especially at high guide vane openings, which eventually can damage the discharge ring of the turbine.

Measurements on the prototype at homologous operation points show a similar behavior in time and frequency domains, regards some differences that can be attributed to scale effects, as previously explained.

The envelope of the acceleration proved to be able to preserve the frequencies of the rsi, both in the model and in the prototype, with sufficiently high signal-to-noise ratios (>0.01). Particularly, the 25fn spectral component of the envelopes was identified as a powerful indicator of rotor stator interaction. In general, the SNR turned out to be four times larger in the model than in the prototype.

The methodology presented in this paper can be easily applied on prototype since the use of accelerometers is a non-intrusive procedure. This means that its implementation can be carried out using a single portable data logger and a single accelerometer that can be provisionally installed in the laboratory and then in the hydroelectric power plant without disturbing the normal operation of the machines and without compromising the safety of operators and equipment.

Acknowledgement

The authors would like to thank the technical director of Yacretá power station, Eng. Marcelo Cardinali, and the staff of regulation sector for their important contribution.

References

- [1] Rivetti A, Angulo M, Lucino C, Botero F, Liscia S 2017 Hydrodynamic behavior on Kaplan turbines: Experimental methodology for the evaluation of cavitation *Proc. of 3rd Latin American Hydropower & Systems Meeting* (Ecuador)
- [5] International electrotechnical committee 1999 Hydraulic turbines, storage pumps and pump turbines model acceptance tests international standard IEC 60193, 2nd Edition
- [3] Castro A and Botero F 2017 Non-invasive detection of vortex street cavitation *Ing. y Univ.* vol 21 2 <http://www.redalyc.org/articulo.oa?id=47751131004>
- [4] Botero F, Guzmán S, Hasmatuchi V, Roth S. and Farhat M 2012 Flow visualization approach for periodically reversed flows *J. Flow Vis. Image Proces.*
- [5] Bechhoefer E and Kingsley M 2009 A Review of Time Synchronous Average Algorithms *Annual Conference of the Prognostics and Health Management Society*
- [6] Escaler X Egusquiza E Farhat M Avellan F and Coussirat M 2006 Detection of cavitation in hydraulic turbines *Mech. Syst. Signal Process.* vol 20 no 4 983-1007
- [7] Rivetti A Angulo M Lucino C and Liscia S 2014 Mitigation of tip vortex cavitation by means of air injection on a Kaplan turbine scale model *IOP Conf. Ser. Earth Environ. Sci.* vol 22 no 5